INTERNATIONAL JOURNAL OF ENERGY STUDIES

e-ISSN: 2717-7513 (ONLINE); homepage: https://dergipark.org.tr/en/pub/ijes

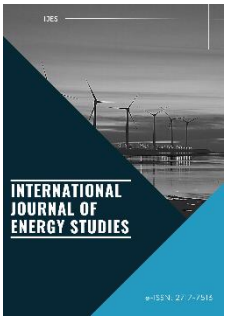

Research Article

Int J Energy Studies 2025; 10(3): 647-676

DOI: 10.58559/ijes.1725711

Received : 23 June 2025

Revised : 03 Aug 2025

Accepted : 12 Aug 2025

Prediction of municipal solid waste quantities using a BiLSTM model, and analysis of biogas and electricity generation potential and greenhouse gas impacts: A case study of Şırnak province

Ceylan Üren[a*], Edip Taşkesen[b]

[a]*Energy Science and Technologies Master's Program, Graduate School of Education, Şırnak University, Şırnak, Türkiye, ORCID: 0009-0009-6474-220X*

[b]*Department of Energy Systems Engineering, Faculty of Engineering, Şırnak University, Şırnak, Türkiye, ORCID: 0000-0002-3052-9883*

*(*Corresponding Author: ceylanlinauren@gmail.com)*

Highlights

- Using the BiLSTM model, municipal solid waste quantities in Şırnak are successfully predicted to increase by 63.9% between 2025 and 2045.
- Biogas production potential estimated by LandGEM rises from 2.47 million m³ in 2025 to 6.86 million m³ in 2045, providing a significant energy source.
- Biogas production is expected to prevent approximately 106,031 tons of CO_2 equivalent greenhouse gas emissions over 21 years, offering environmental benefits.

You can cite this article as: Üren C, Taşkesen E. Prediction of biogas and electricity generation potential from municipal solid waste and analysis of greenhouse gas impacts: A case study of Şırnak province. Int J Energy Studies 2025; 10(3): 647-676.

ABSTRACT

This study focuses on predicting the Municipal Solid Waste (MSW) quantities in Şırnak province for the 2025-2045 period using a BiLSTM deep learning model, and analyzes the related Biogas (methane gas, CH_4), Electricity Energy Produciton Potential (EEPP), and Greenhouse Gas (GHG) emissions based on these predictions. The model was developed using a dataset of 12 financial, social, and demographic variables with an 80% training and 20% testing split, implemented in Python with the NumPy library. Trained on data from 2007 to 2024, the model achieved a low Mean Absolute Percentage Error (MAPE) of 3.83% after hyperparameter optimization, with an average MAPE of 7.99% from k-fold cross-validation. MAPE values below 10% indicate high accuracy and reliability. Findings suggest that the MSW amount, approximately 298,090 tons in 2025, will increase to around 825,929 tons by 2045, representing a 63.9% rise driven mainly by rapid urbanization, population growth, and economic development. Using LandGEM software, CH_4 production potential was estimated at about 2.47 million m³ in 2025 and 6.86 million m^3 in 2045. Assuming 75% effective CH_4 collection, 1.85 million m³ and 5.14 million m³ of CH_4 could be recovered in 2025 and 2045, respectively. Corresponding electricity generation potentials are 5,157 MWh in 2025 and 14,315 MWh in 2045, with a total of 225,478 MWh predicted over 21 years. The optimal required plant capacity is calculated as 1.63 MW. Additionally, approximately 141,375 tons of CO_2 equivalent GHG emissions are expected to be avoided over this period. These results highlight the environmental benefits of replacing fossil fuels with biogas. The study concludes that BiLSTM based MSW predictions provide a reliable tool for waste management and energy planning, supporting sustainable environmental policies and strategic decision making.

Keywords: Deep learning, BiLSTM, Waste, Energy, Environment

1. INTRODUCTION

Nowadays, increasing population, urbanization, and changes in consumption habits cause the amount of MSW to increase day by day. This situation necessitates the reconsideration of waste management policies within the framework of sustainability principles. It is of great importance not only to dispose of solid waste but also to convert it into useful outputs such as energy production in order to reduce environmental impacts. Especially, electricity obtained through biogas production promotes the use of renewable energy sources and contributes to the reduction of Greenhouse Gas (GHG) emissions [1-5].

When MSW naturally decomposes and is processed, it emits GHG'es such as Carbon dioxide (CO2) and CH4. Although cities cover only about 2% of the earth's surface, the large amounts of MSW generated in cities constitute approximately 70% of global GHG emissions. Furthermore, poor waste disposal methods such as open dumping and open burning significantly contribute to global warming. Worldwide, the amount of MSW is projected to exceed 2.2 billion tons in 2025 and 3.4 billion tons in 2050. The World Health Organization (WHO) estimates that about 97% of cities with populations over 100,000 in low and middle income countries usually dispose of their waste in dumpsites [6].

MSW is collected from various sources such as industrial facilities, manufacturers, households, schools, offices, markets, and shops. MSW may contain a variety of organic and inorganic materials, including polymers and non-renewable substances, or mixtures thereof [7, 8]. MSW components can be classified into seven main groups: organics, paper/cardboard, plastics, glass, metals, textiles, and inert materials. Remaining components are grouped as miscellaneous (others) [8, 9]. The pie chart in Figure 1-a shows the proportional distribution of these components according to ASTM D5231 standard. A more detailed sub-classification of MSW components is presented in the tree diagram in Figure 1-b.

The composition of MSW varies according to source location, economic status, industrial structure, lifestyle, and applied waste management methods. Knowing the quantity and characteristics of MSW is important both for facilitating processing and optimizing energy recovery through appropriate waste to energy methods. Especially, calorific value and physicochemical properties play a critical role in achieving high energy efficiency and obtaining harmless waste. In developing countries, the majority of MSW originates from household sources

(55-80%) and is highly heterogeneous in content, making it difficult to determine suitable processing methods. Therefore, steps such as pre-sorting and public awareness are important for effective waste management. However, current methods such as landfilling and incineration, widely applied in many countries, pose serious long-term risks to the environment and human health. Leachate induced soil and water pollution, as well as air pollution caused by burning, are particularly concerning [8]. Insufficient landfill areas create an additional problem in urban settings. Other significant environmental and health impacts related to MSW are presented in Figure 2.

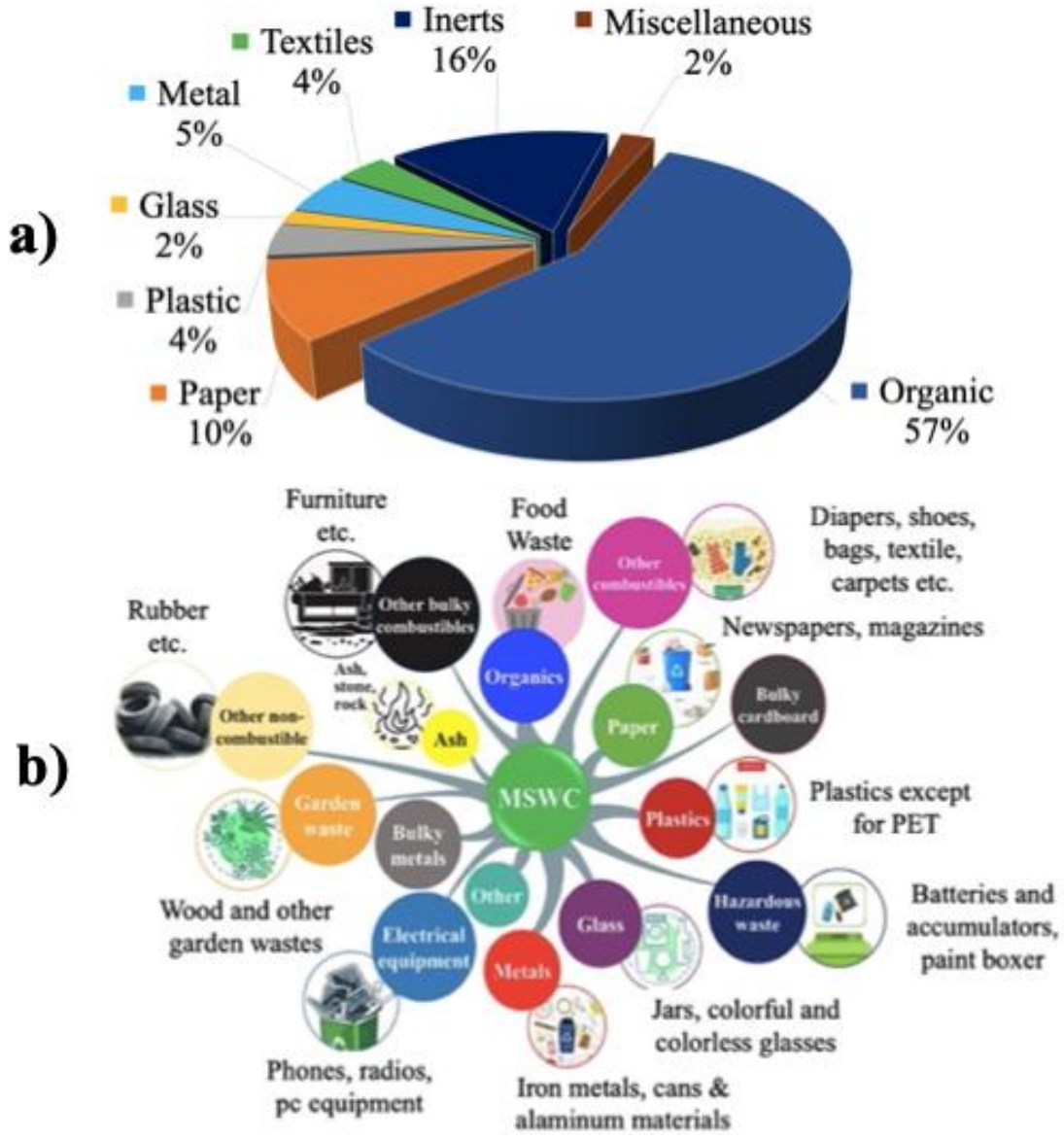

Figure 1. Characterization of MSW (MSW): (a) Global composition of MSW based on ASTM D5231 standard; (b) Detailed classification of MSW components (MSWC mapping) [8].

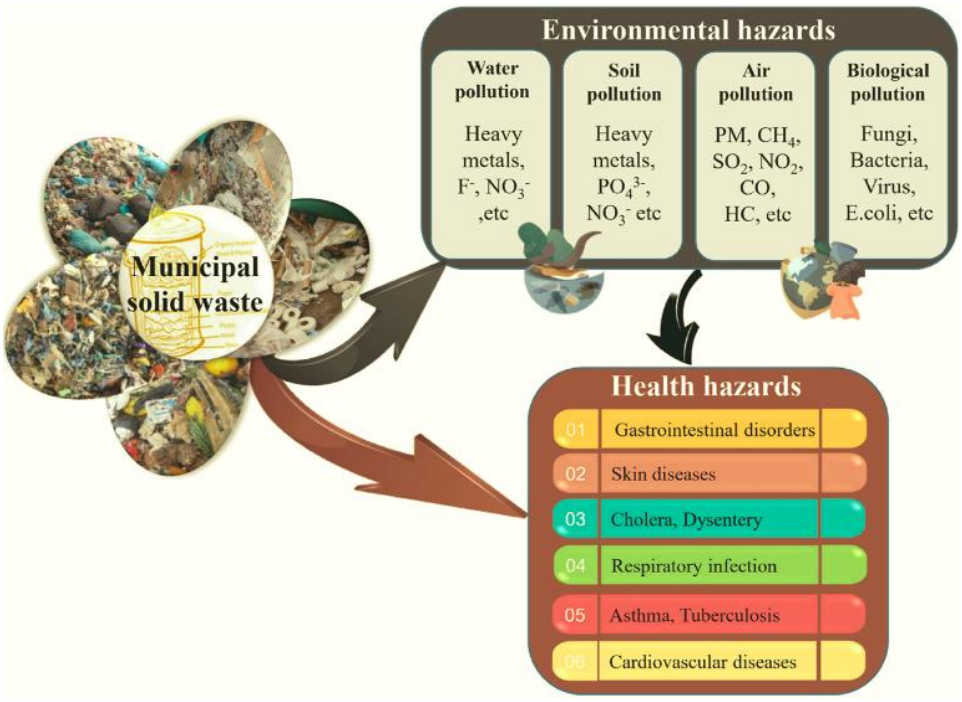

Figure 2. Effects of MSW on human health and the environment [8, 10].

Methods such as incineration, pyrolysis, gasification, anaerobic digestion, biomethanation, and landfill gas recovery are used for energy production from MSW. These methods aim both to reduce waste volume and to generate energy. Biochemical conversion is a process where biomass is broken down by microorganisms; however, it requires high investment and precise control due to its low efficiency. Landfilling is one of the most common and traditional methods; landfill gas formed by natural digestion can be converted into energy, but its quality is low due to low CH_4 content and corrosive components. Although landfilling is simple, low cost, and widely accessible, it is criticized for its high land requirement and low sustainability. In terms of energy production, landfilling is less efficient than anaerobic digestion and must be carefully evaluated considering social acceptance and environmental impacts [8, 11, 12].

The landfill system aims to dispose of MSW in a controlled way by burying it underground. Waste is spread in layers in specially prepared areas, compacted, and covered with soil to minimize contact with the environment. As waste biologically decomposes in an oxygen free (anaerobic) environment, various gases (especially CH_4 and CO_2) are produced. This gas mixture, called "landfill gas," is collected via special pipes and wells and used for energy production in the form of biogas. The landfill process consists of four main biochemical stages: initial acclimation phase, acid phase, CH_4 production phase, and maturation phase. In addition, leachate forms and is

controlled with liner systems, drainage pipes, and treatment units to prevent environmental damage. This process reduces waste volume and limits environmental adverse effects [8]. Figures 3 illustrate the processes and components related to the landfill system.

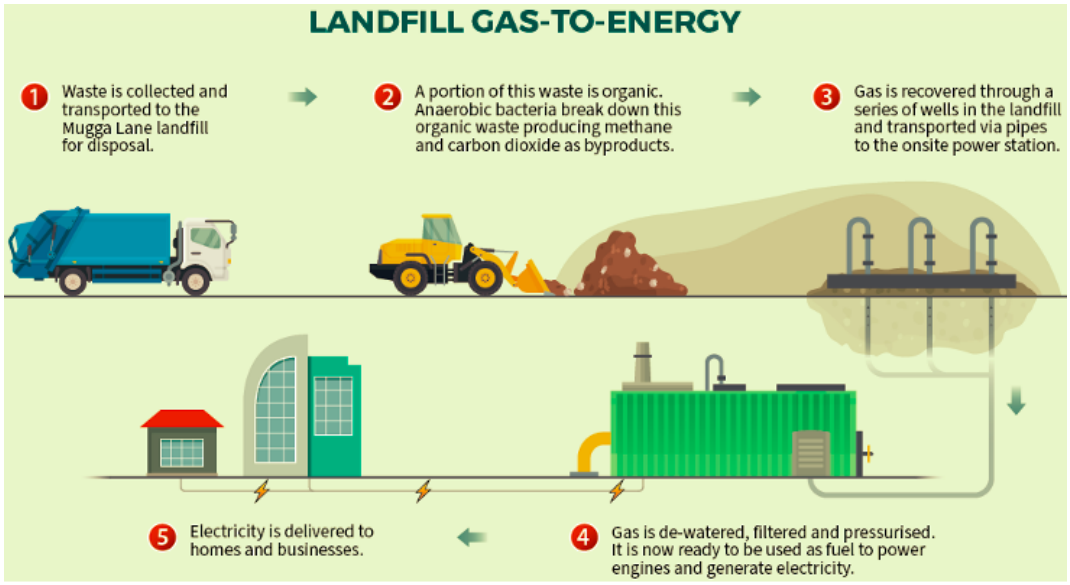

Figure 3. Electricity Energy Production (EEP) process using the landfill system and its key components [13].

Accurate prediction of solid waste amounts is a critical necessity for developing sustainable waste management strategies, effective resource utilization, and minimizing environmental impacts. Especially, forecasting changes in MSW quantities allows for effective decisions in waste collection, transportation, and disposal planning, as well as in recycling and energy recovery applications.

In recent years, Deep Learning (DLr) techniques, particularly for analyzing time series data, have been increasingly used in MSW prediction models due to their superior performance. Long Short Term Memory (LSTM) networks analyze the temporal change structure of past data to provide accurate future predictions [14-20]. In this context, the Bidirectional LSTM (BiLSTM) model is an advanced method that improves prediction accuracy by analyzing data both forward and backward in time [6, 21].

The LSTM cell is a special type of artificial neural network unit that can selectively remember and forget information over time. The current input data, the previous hidden state, and the previous

cell state are processed together. The forget gate decides which information to discard, while the input gate determines how much new information to add. The cell state is updated accordingly, and the output gate defines the new hidden state. In this way, LSTM can learn long-term dependencies while adapting to new information. It also significantly reduces vanishing and exploding gradient problems commonly seen in classical Recurrent Neural Networks (RNNs) [22-25].

BiLSTM, on the other hand, is an advanced LSTM model that operates bidirectionally one layer processes the data forward, while the other processes it backward. This allows for more comprehensive and accurate predictions by considering both past and future contextual information. The two directional hidden state vectors are combined to form the final output. BiLSTM provides higher performance than classical RNNs and unidirectional LSTMs in applications where understanding bidirectional context is critical, such as language modeling, sentiment analysis, and time series forecasting [6, 26, 27].

In this study, MSW quantities for Şırnak province in the Southeastern Anatolia Region of Turkey between 2007 and 2024 were evaluated together with financial, social, and demographic indicators, and predicted using the BiLSTM DLr model. Based on the predictions, the biogas production potential, EEP, and GHG emissions resulting from the waste amounts were analyzed. Thus, the sustainability of waste management strategies in terms of environmental impacts and energy recovery potential were demonstrated. The aim of the study is to accurately predict MSW quantities using the BiLSTM DLr model and to contribute to sustainable waste management and energy recovery strategies by analyzing biogas production potential, EEP, and GHG emissions based on these predictions.

2. MATERIALS AND METHODS

2.1. Study Area

Şırnak is located in the Southeastern Anatolia Region of Türkiye, bordered by Iraq to the south, Mardin to the west, Siirt to the north, and Hakkâri to the east. The province consists of seven districts, with a total area of 7,172 km^2 and an average elevation of 1,400 meters [28]. According to data from the Turkish Statistical Institute (TÜİK), the total population of Şırnak was 416,001 in 2007 and increased to 570,826 by 2024. MSW quantities in Şırnak between the years 2007 and 2024 were analyzed. The MSW data were obtained from TÜİK, and the annual total collected

waste amounts are presented in Table 1 [29]. These data were used to train the model and to evaluate its prediction performance. Figure 4 shows the characterization and percentage distribution of the MSW types in Şırnak.

Table 1. Annual MSW quantities collected in Şırnak Province from 2007 to 2024 [29].

Year	MSW (Tons)	Year	MSW (Tons)
2007	44,673	2016	131,621
2008	51,821	2017	139,255
2009	63,725	2018	183,133
2010	71,821	2019	207,238
2011	88,544	2020	211,676
2012	90,709	2021	217,716
2013	66,658	2022	228,602
2014	109,923	2023	240,032
2015	118,936	2024	252,033

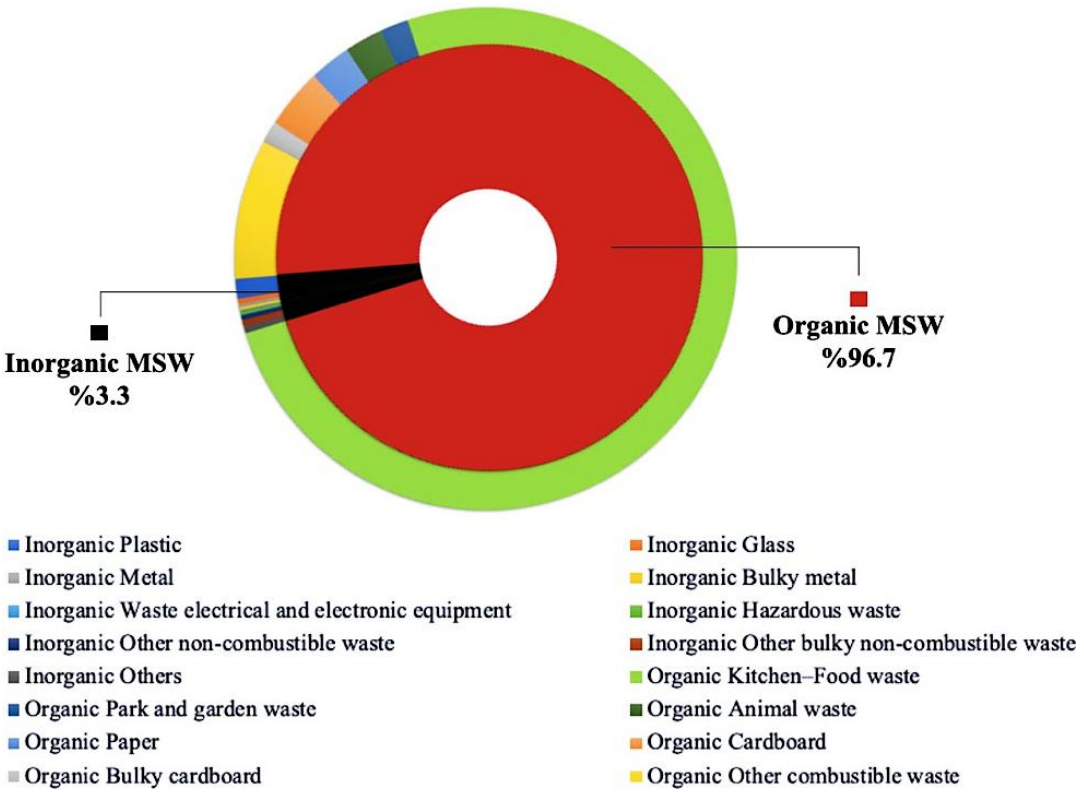

Figure 4. MSW characterization and percentage distribution of waste types [30].

2.2. BiLSTM Based MSW Prediction Model Approach

LSTM offers an effective method for MSW prediction by considering both dynamic and static variables [6, 31]. LSTM is an improved version of classic RNNs with feedback architecture that can learn long-term dependencies in sequential data. LSTM networks are widely used especially

in time series forecasting, speech recognition, handwriting analysis, and network traffic applications. The fundamental unit of this architecture, the LSTM cell, consists of a cell state and three gates (input, forget, and output gates). These gates determine when and how much information enters or leaves the cell and what portion is forgotten [22-25]. Figure 5 shows the LSTM structure.

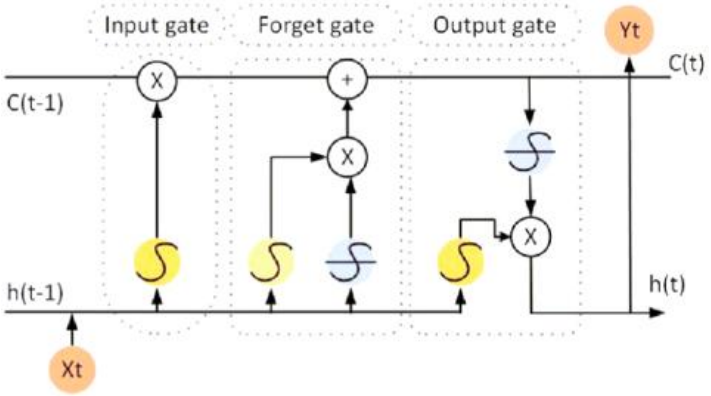

Figure 5. LSTM cell structure [6].

The working principle of the LSTM cell shown in Figure 5 can be summarized as follows: The current input data to the cell, x_t, previous hidden state h_{t-1}, and previous cell state C_{t-1} are evaluated together. First, the forget gate (f_t) decides which information to discard from the cell. Then, the input gate (it) determines how much new information is added to the cell. The candidate cell state (C_t) is created via the tanh activation function. The cell state C_t is updated by forgetting some previous information and adding new information. Finally, the output gate (o_t) determines the new hidden state (ht), which is calculated by multiplying the output gate with the tanh of the updated cell state C_t. This way, the LSTM cell can learn and maintain long-term dependencies while adapting to new information. LSTMs significantly mitigate problems common in classical RNN's such as vanishing and exploding gradients. Mathematically, this process is expressed as follows [23, 24, 32]:

- Input gate i_t:

$$i_t = \sigma(W_i \times [h_{t-1}, x_t] + b_i) \quad (1)$$

- Forget gate f_t:

$$f_t = \sigma(W_f \times [h_{t-1}, x_t] + b_f) \quad (2)$$

- Output gate o_t:

$$o_t = \sigma(W_o \times [h_{t-1}, x_t] + b_o) \quad (3)$$

- Cell state C_t:

$$C_t = f_t \times C_{t-1} + i_t \times \tanh(W_c[h_{t-1}, x_t] + b_c) \quad (4)$$

- Hidden state h_t:

$$h_t = o_t \times \tanh(C_t) \quad (5)$$

Here, σ represents the sigmoid activation function, and tanh is the hyperbolic tangent function. W denotes weight matrices and b indicates bias terms. The gate vectors have the same dimension as the hidden state vector h_t. LSTM networks typically use sigmoid and tanh functions together to effectively control information flow.

Figure 6 illustrates the BiLSTM structure, an enhanced version of ordinary LSTM networks that provides more comprehensive learning by considering both past (previous) and future (next) contextual information in time series data. BiLSTM essentially consists of two separate LSTM layers: one processes the input forward (left to right), and the other processes it backward (right to left). The outputs of both LSTM layers are combined at each time step (usually by concatenation, summation, or multiplication) to produce the final output. This bidirectional architecture enables BiLSTM to access not only past states but also future states, learning a richer contextual representation. The input sequence xt is fed separately to both forward LSTM ($\overrightarrow{h_t}$) and backward LSTM ($\overleftarrow{h_t}$). The resulting two directional hidden state vectors are concatenated to form the total output $h_t = [\overrightarrow{h_t}; \overleftarrow{h_t}]$. This structure provides significant advantages in tasks where understanding both directions of context is critical, such as language modeling, sentiment analysis, biomedical signal processing, and time series forecasting. BiLSTM surpasses limitations of classic RNNs and

unidirectional LSTMs by offering higher accuracy in sequential data prediction and classification [6, 26, 27].

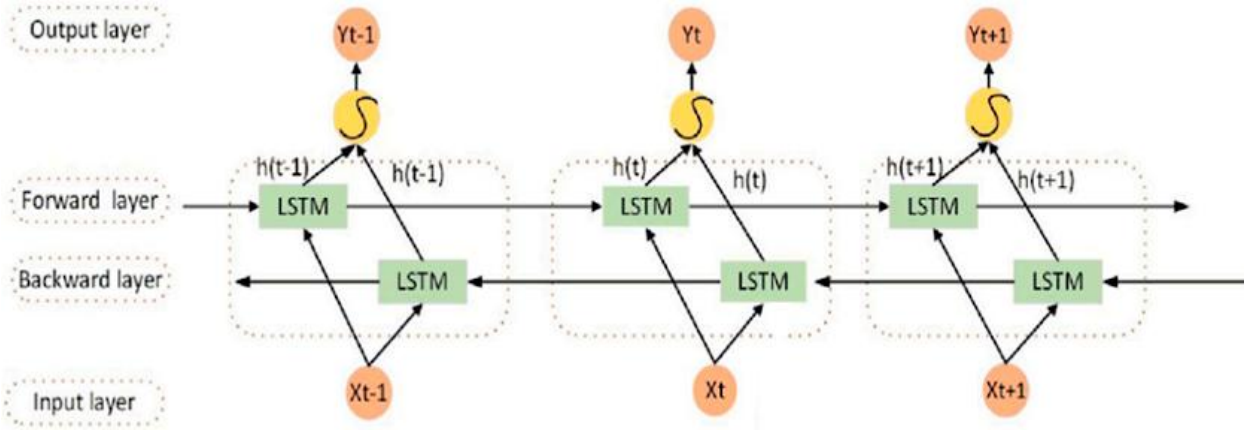

Figure 6. BiLSTM Cell Structure [6].

In this study, a BiLSTM based model developed by Liu et al. (2024) [6] was applied. The BiLSTM architecture produces more accurate predictions through bidirectional LSTM layers that process the input sequence both forward and backward [6, 33, 34].

As shown in Figure 7, the BiLSTM neural network consists of two separate LSTM layers processing time series data in both forward and backward directions. In this structure, hidden vectors performing forward (past) and backward (future) computations are combined to yield a more comprehensive output [6, 33, 34]. The horizontal axis represents the bidirectional flow of the time series; the vertical axis shows the unidirectional flow from the input layer to the hidden layer and then to the output layer. The final output is denoted as y_t. The LSTM cell structure includes input, hidden, and output layers. The "+" and "×" symbols represent addition and multiplication operations, respectively. The inputs of each memory unit at time ttt are as follows [6]:

- X_t: input data at time t,
- $H_t - 1$: hidden layer output at time t−1,
- $C_t - 1$: data stored in the memory cell at time t−1,
- H_t: hidden layer output at time t,
- C_t: memory cell state at time t.

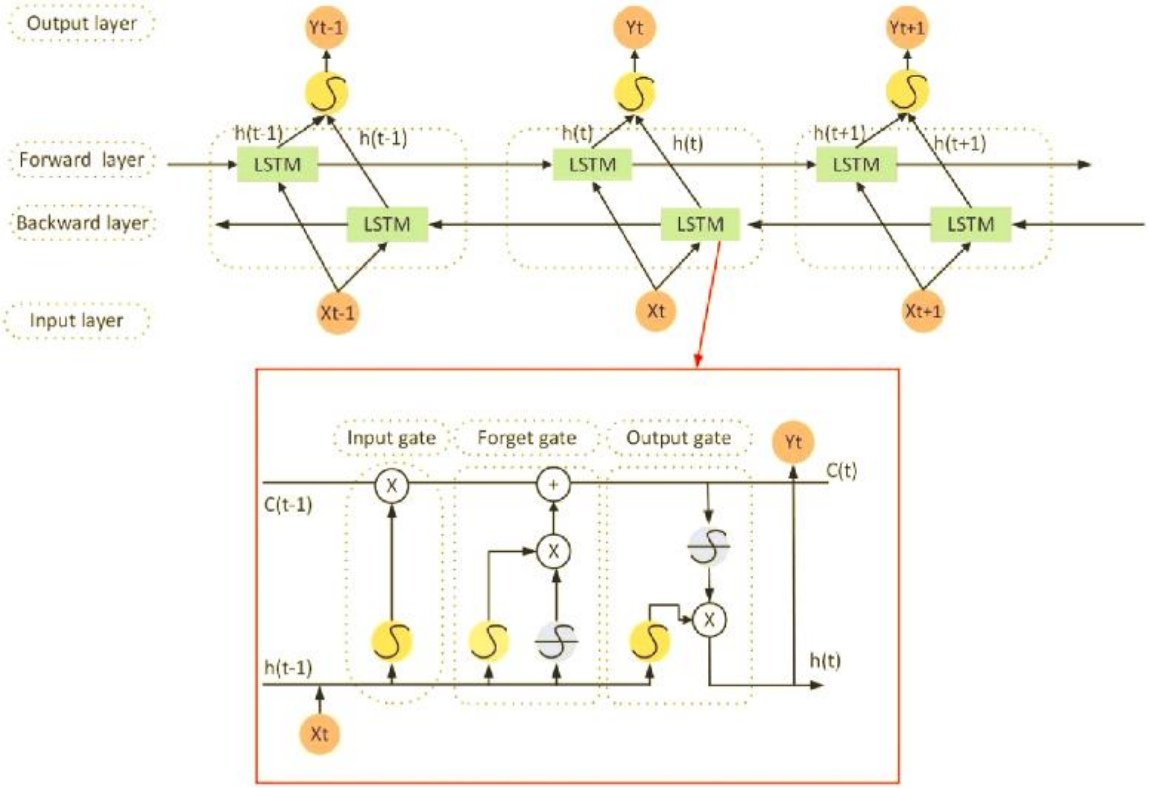

Figure 7. BiLSTM model architecture [6].

The BiLSTM model processes time series data in both forward and backward directions, providing bidirectional information flow. Information flow in each LSTM cell is controlled by three main gates: the input gate, forget gate (f_t), and output gate (O_t). These gates operate according to the following equations [6]:

$$i_t = \sigma(W_i \times [H_t - 1, X_t] + b_i) \quad (6)$$

$$f_t = \sigma\left(W_f \times [H_t - 1, X_t] + b_f\right) \quad (7)$$

$$o_t = \sigma(W_o \times [H_t - 1, X_t] + b_o) \quad (8)$$

Model parameters were determined through preliminary testing. Here, W_f, W_i, W_o represent the weight vectors of the forget, input, and output gates, respectively; and b_f, b_i, b_o are their bias vectors [6]. The model was implemented using Python 3.12.3 and the NumPy library. Data were split into 80% training and 20% testing sets and processed in .csv format. The control variable

method was applied by changing only one parameter in each model run, and the prediction performance was evaluated.

The dataset consists of 12 variables from financial, social, and demographic domains. Training data were used for model learning, while test data evaluated general performance. To avoid overfitting, part of the training data was set aside as a validation set, and the model's performance on different datasets was objectively assessed using cross validation [6, 35, 36]. As illustrated in Figure 8, the dataset was divided into K equal parts; in each iteration, one part was used as test data and the remaining K−1 parts as training data. This process was repeated K times. In this study, K=5 and five experiments were conducted. The training:test ratio in each experiment was 4:1. The model's general fit to small samples was assessed via average MAPE, RMSE, and MAE values from these five experiments. Mean Absolute Percentage Error (MAPE) was also used as a control metric. The three evaluation criteria MAPE, Root Mean Square Error (RMSE), and Mean Absolute Error (MAE) measure the model's ability to predict and fit the data. MAPE is interpreted as follows:

- MAPE ≤ 10%: High accuracy,
- 10% < MAPE ≤ 20%: Good accuracy,
- 20% < MAPE ≤ 50%: Acceptable accuracy,
- MAPE > 50%: Low accuracy.

MAPE, RMSE, and MAE are calculated by the following equations 9, 10, and 11 respectively [6]:

$$MAPE = \frac{100\%}{n}\sum_{i=1}^{n}\left|\frac{\hat{y}-y_i}{y_i}\right| \tag{9}$$

$$RMSE = \sqrt{\frac{1}{n}\sum_{i=1}^{n}(\hat{y}-y_i)^2} \tag{10}$$

$$MAE = \frac{1}{n}\sum_{i=1}^{n}|\hat{y}-y_i| \tag{11}$$

Where:

- $\hat{y}$ = predicted value,
- y_i = actual value,
- n = number of data points.

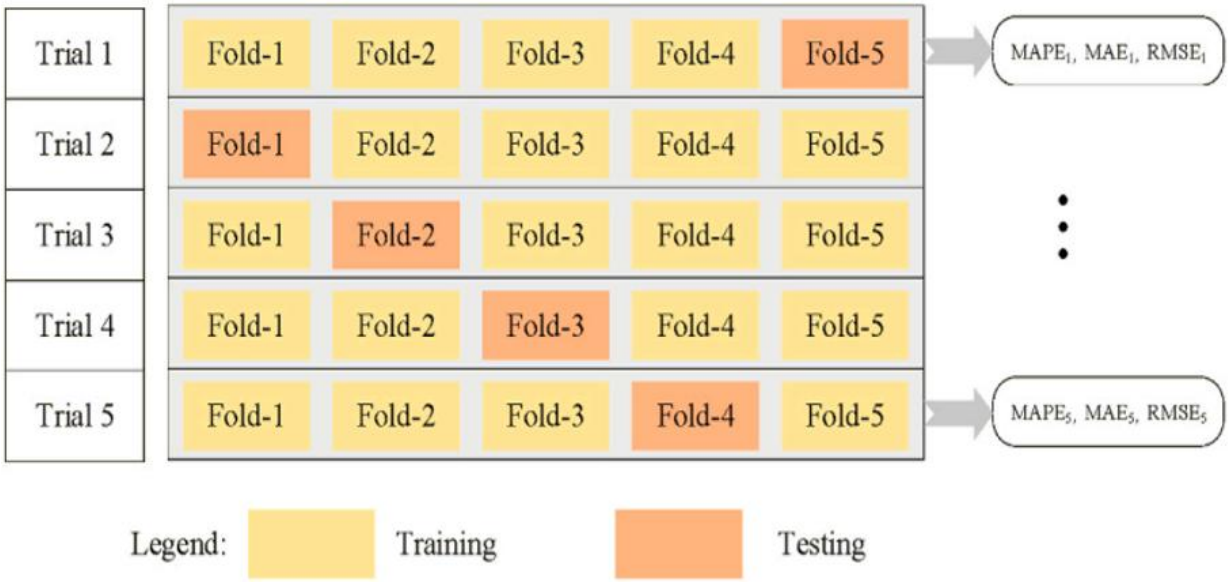

Figure 8. K-fold cross validation [6].

This study used 12 variables identified in the literature and separated into 80% training and 20% testing sets. The selected variables relate to financial, social, and demographic indicators identified as linked to MSW generation in previous studies [6, 37, 38]. The dataset contains 228 observations including GDP, per capita consumption expenditure, per capita disposable income, service sector size, fixed capital investment, passenger transportation, passenger traffic, urban road area, number of incoming tourists, urban population, resident population, and urban population density. These data were compiled from the Şırnak Statistical Yearbook published by the Turkish Statistical Institute (TÜİK) for 2007-2024 (Table 2) [29]. The model was trained on data from 2007-2019 and tested with data from 2020-2024. The relationship between MSW and the variables was evaluated using grey relational analysis, and the two most correlated variables from each group were selected as model input parameters. Descriptive statistics for the dataset including Time Step, Hidden Layer, Batch Size, Learning Rate (Lr), Epoch, and MAPE (%) were evaluated. Additional descriptive statistics such as mean, median, standard deviation, maximum, and minimum values were provided to better reflect variable characteristics.

Table 2. Annual data of financial, social, and demographic indicators used in the msw prediction model (Şırnak, 2007-2024) [29].

Year	Gross Domestic Product (GDP) (TRY)	Per Capita Consumption Expenditure of Urban Households (TRY)	Per Capita Disposable Income (TRY)	Fixed Capital Investment (TRY)	Total Value of Service Sector (TRY)	Passenger Turnover Rate (times)	Passenger Traffic (thousands)	Number of Incoming Tourists (thousands)	Urban Road Area (km²)	Urban Population (persons)	Resident Population (persons)	Urban Population Density (persons/km²)
2007	336,281,250	228	681	5E+10	1E+10	155.15	10,860.4	2,985	0.47	54,302	416,001	58
2008	312,562,500	212	633	5E+10	1E+10	169.81	11,887	3,466	0.49	59,435	429,287	60
2009	325,125,000	220	659	5E+10	1E+10	181.90	12,732.8	5,354	0.49	63,664	430,424	60
2010	350,250,000	237	710	5E+10	1E+10	155.04	10,852.6	4,398	0.49	54,263	430,109	60
2011	400,500,000	272	811	5E+10	1E+10	175.24	12,267	5,384	0.52	61,335	457,997	64
2012	401,000,000	272	813	5E+10	1E+10	180.85	12,659.6	12,139	0.53	63,298	466,982	65
2013	462,000,000	313	936	5E+10	1E+10	172.16	12,051	11,249	0.54	60,255	475,255	66
2014	804,000,000	545	1,629	5E+10	1E+10	180.13	12,609.4	1,296	0.55	63,047	488,966	68
2015	1,608,000,000	1,090	3,258	5E+10	1E+10	181.05	12,673.4	12	0.55	63,367	490,184	68
2016	3,216,000,000	2,180	6,516	5E+10	1E+10	154.38	10,806.4	23	0.54	54,032	483,788	67
2017	4,019,000,000	2,725	8,143	2E+11	3E+10	157.01	10,991	7,206	0.57	54,955	503,236	70
2018	9,317,000,000	6,317	18,878	3E+11	5E+10	179.32	12,552.2	30,435	0.59	62,761	524,190	73
2019	10,612,000,000	7,195	21,502	4E+11	7E+10	176.39	12,347.6	123,983	0.60	61,738	529,615	74
2020	11,313,000,000	7,670	22,922	4E+11	7E+10	183.39	12,837	130,351	0.61	64,185	537,762	75
2021	14,267,000,000	9,673	28,908	5E+11	9E+10	193.32	13,532.4	203,164	0.62	67,662	546,589	76
2022	15,535,000,000	10,532	31,477	5E+11	9E+10	198.25	13,877.6	217,062	0.63	69,388	557,605	77
2023	16,955,000,000	11,495	34,354	6E+11	1.1E+11	216.95	15,186.4	239,004	0.64	75,932	570,745	79
2024	18,468,000,000	12,521	37,420	7E+11	1.3E+11	209.47	14,663	243,871	0.64	73,315	570,826	79

2.3. Calculation of CH_4 and Electricity Energy Production Potential and Plant Installed Capacity

In this study, based on the predicted amounts of MSW for the period 2025-2045, the volume of CH_4 gas that can be obtained from sanitary landfill sites was analyzed. CH_4 production was estimated using version 3.1 of the Landfill Gas Emission Model (LandGEM), considering the annual waste input (Figure 9) [39, 40].

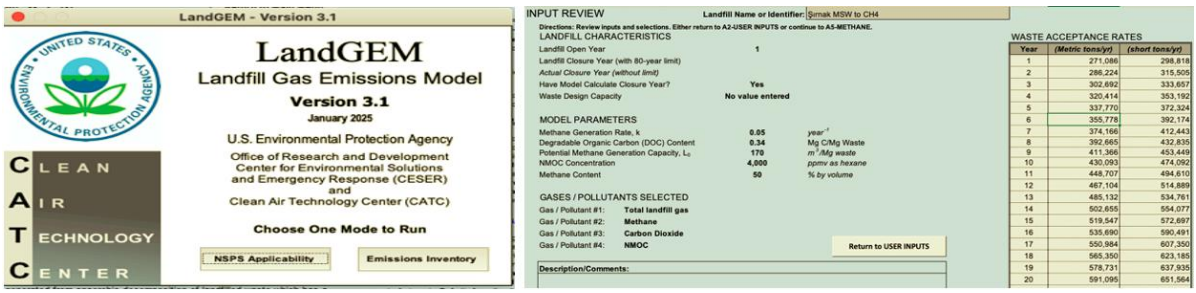

Figure 9. CH_4 gas volume analysis using LandGEM v3.1 based on projected MSW quantities.

The model is based on a first order decay equation. The annual CH_4 gas production (GP_{CH_4}) is calculated using Equation 12 [39, 40]:

$$GP_{CH_4}(y) = \sum_{i=1}^{y} \sum_{j=0.1}^{1} kL_0 \times \left(\frac{MSW_{(LF)}}{10}\right) \times e^{-kt_{ij}} \quad (12)$$

Where:

- $GP_{CH_4}(y)$: total CH_4 gas produced in year y (m^3/year),
- i: 1 year time interval,
- y: difference between the calculation year and the waste acceptance year,
- j: 0.1 year time interval,
- k: CH_4 production rate constant (0.05 $year^{-1}$),
- L_0: potential CH_4 gas production capacity (170 m^3/ton),
- $MSW_{(LF)}$: annual amount of MSW disposed in sanitary landfills in the province (ton/year),
- t_{ij}: age of the j-th fraction of waste in year i.

In practice, not all CH_4 gas produced at landfill sites can be collected for Electricity Energy Production (EEP). In this study, based on Ref. [40-44], a CH_4 gas collection efficiency of 75% was assumed. Accordingly, the amount of CH_4 gas available for EEP is Capturable CH_4 (CAP_{CH_4}) calculated using Equation 13 [40]:

$$CAP_{CH_4} = GP_{CH_4} \times 0.75 \quad (13)$$

The electricity energy production potential (EEPP) from the collected CH_4 is calculated annually using Equation 14 [40, 42, 44]:

$$EEPP_{CH_4} = \frac{CAP_{CH_4}(y) \times 37.2 \times \partial \times 0.9 \times \in}{\emptyset} \quad (14)$$

Where:

- $EEPP_{CH_4}$: Electricity energy production potential (MWh),
- 37.2: calorific value of CH_4 gas (MJ/m^3) [40, 44],
- ∂: capacity factor (%85) [40, 44, 45],

- 0.9: oxidation correction factor [40, 44],
- ∈: EEP efficiency in biogas power plant (%35) [40, 44],
- ∅: conversion factor from MJ to MWh (3600 MJ/MWh).

The CH_4 gas producible from MSW in Şırnak between 2025 and 2045, and the electricity energy obtainable from this gas, serve as the basis for capacity planning of energy production facilities to be established. The EEPP, varying annually in parallel with increasing waste quantities, should be considered in scaling Biogas Plants (BP). Accordingly, assuming continuous operation of the facility throughout the year on a 24 hour basis, the required installed capacity is calculated using Equation 15 [40]:

$$BPPC = \frac{EP_{LFG}}{D_{hr} \times \gamma} \quad (15)$$

Where;

- $BPPC$: installed capacity of the biogas power plant (MW),
- D_{hr}: daily operating hours (24 hours),
- γ: number of days in the year (365 days).

This method was used to estimate the CH_4 and EEPP based on the projected MSW quantities in Şırnak between 2025 and 2045.

2.4. Analysis of the Impact on GHG Emissions

In this study, GHG emissions resulting from biogas based. production from MSW projected for Şırnak province between 2025 and 2045 were analyzed. The calculations were based on the carbon dioxide equivalent (CO_2eq.) emission estimation method for energy production recommended by the Intergovernmental Panel on Climate Change (IPCC), using emission factor (EF) data associated with the fuels used in the production technologies [46].

The projected emission values were expressed in CO_2eq. and estimated separately for each year. In addition, GHG emissions that would be produced if the same amount of electricity were generated using fossil fuel sources such as natural gas ($NGCO_2$eq.), oil (OCO_2eq.), and coal (CCO_2eq.) were also calculated and compared with MSW biogas based EEP (BCO_2eq). Based on

this comparison, the potential contribution of biogas use to reducing GHG emissions was evaluated.

GHG emissions in CO_2eq. terms were calculated using the IPCC recommended method and average EFs obtained from various sources [46-49]:

$$\mathrm{CO_2}eq. = \mathrm{EEP} \times \mathrm{EF} \quad (16)$$

Where:

- CO_2eq.: Annual total CO_2 equivalent emissions (ton CO_2eq./year),
- EEPP: Electricity energy production potential (MWh/year)
- EF: Emission factor determined according to the production technology (ton CO_2eq./MWh). Table 3 presents the average EFs for EEP sources including biogas, natural gas, oil, and coal.

Table 3. EFs by EEP Sources [46-49].

EEP Source	Unit	EF		
		Min.	Average	Max.
Biomass (MSW biogas)	Ton CO_2eq./MWh	0.030	0.050	0.101
Natural Gas	Ton CO_2eq./MWh	0.410	0.490	0.650
Oil	Ton CO_2eq./MWh	0.547	0.733	0.935
Coal	Ton CO_2eq./MWh	0.756	0.888	1.310

Furthermore, the average annual amount of CO_2eq. emissions that could be avoided by using MSW biogas instead of fossil fuels was estimated (B. Avg. Avod. $\mathrm{CO_2}$eq.). This was calculated by comparing the CO_2eq. from biogas production (BCO_2eq.) with the CO_2eq. emissions from alternative sources like coal (CCO_2eq.), oil (OCO_2eq.), and natural gas ($NGCO_2$eq.), using the following equation:

$$B.Avg.Avod.CO_2eq. = \frac{(NGCO_2eq. - BCO_2eq.) + (OCO_2eq. - BCO_2eq.) + (CCO_2eq. - BCO_2eq.)}{3} \quad (17)$$

Where:

- B.Avg. Avoided CO_2eq.: CO_2eq. emissions avoided annually by using biogas for EEP,
- BCO_2eq.: CO_2eq. from biogas based EEP,
- $NGCO_2$eq.: CO_2eq. from natural gas based EEP,
- OCO_2eq.: CO_2eq. from oil based EEP,
- CCO_2eq.: CO_2eq. from coal based EEP.

3. RESULTS AND DISCUSSION

3.1. MSW Forecasting Results Using the BiLSTM Model

In this study, a DLr based BiLSTM model was employed to forecast the amount of MSW in Şırnak province for the period 2025-2045. To optimize prediction accuracy, four parameters were adjusted during the operation of the neural network model: Lr, time step, number of hidden neurons in each layer, and the number of training epochs. A control variable method was used to select the best prediction model, in which only one parameter was changed at a time.

To enhance model performance, different combinations of hyperparameters were tested. The configuration that achieved the lowest MAPE was determined as: Time Step=3, Hidden Layer=128, Batch Size=8, Lr=0.001, and Epoch=100. Using this structure, the average MAPE value was calculated to be 3.83% (Table 4). This result indicates that the model operates with high accuracy and can be reliably used for future forecasting.

Table 4. Parameter combinations tested for the BiLSTM model and corresponding MAPE performances.

Time Step	Hidden Layer	Batch Size	Lr	Epoch	MAPE (%)
3	64	8	0.001	100	8.25
3	128	16	0.001	150	6.72
3	32	16	0.005	100	12.84
3	64	32	0.0005	200	7.11
3	128	8	0.001	150	5.93
3	128	8	0.001	100	3.83

To further test the accuracy, validity, and general performance of the model on different data subsets, K-fold cross-validation was performed with K=5. According to the results, the best performance was achieved in the 5th iteration with a MAPE of 5.36%, while the worst performance occurred in the 3rd iteration with a MAPE of 13.21%. The average MAPE value was 7.99%, and since it is below 10%, the model is considered to have high accuracy (Table 5).

Table 5. K-fold cross validation results (K=5) and model performance metrics.

Fold	MAE	MAPE (%)	RMSE
Fold 1	62.45	7.33	70.12
Fold 2	48.90	5.65	54.73
Fold 3	89.77	13.21	101.35
Fold 4	67.92	8.41	76.88
Fold 5	46.15	5.36	50.67

Figure 10 presents the forecasting results graphically using the BiLSTM model developed in Python. In the figure, actual MSW generation data from 2007 to 2024 (blue line), training predictions for 2007-2019 (orange line), test predictions for 2020-2024 (green line), and future forecasts for 2025-2045 (red line) are shown.

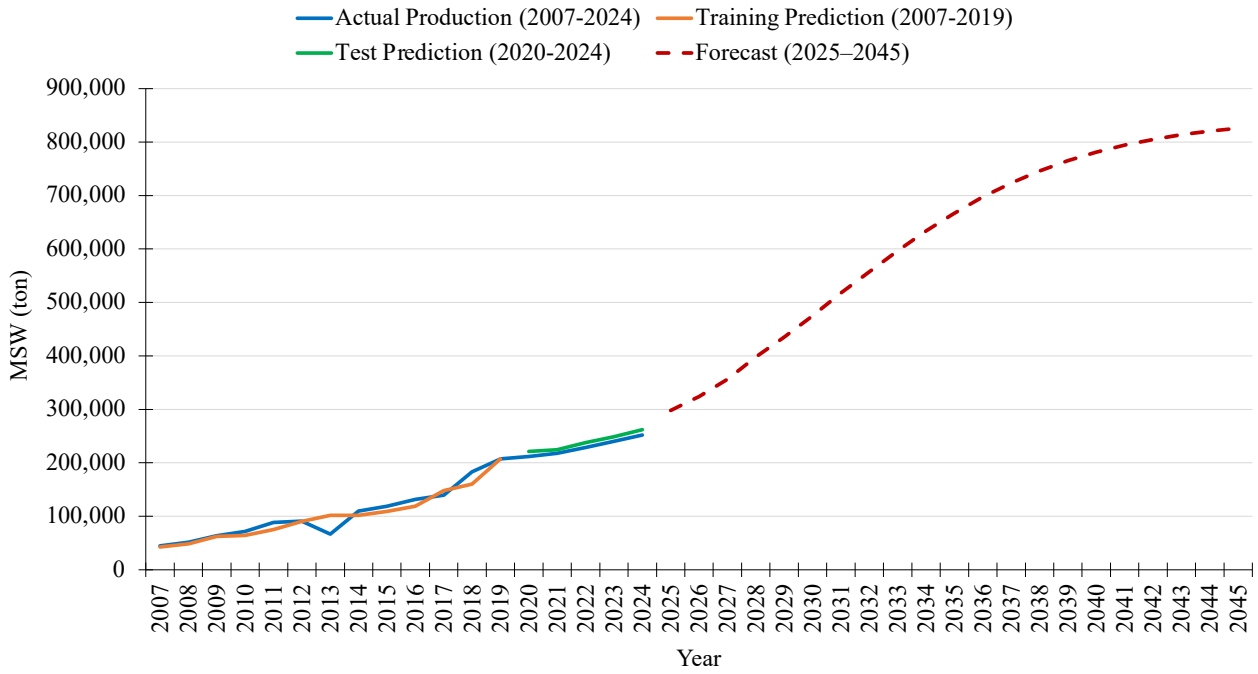

Figure 10. Actual, training, test, and future predicted MSW quantity results for the 2007-2045 period using the BiLSTM model.

Upon examining these findings, it is observed that the training predictions for 2007-2019 are very close to actual values. The resulting predictions yielded MAPE values below 3.83%, showing strong agreement with real data. This indicates that the BiLSTM architecture effectively learns from time series data. Moreover, the test period predictions (2020-2024) also align well with actual production trends, demonstrating that the model has a strong generalization capability and can perform well in forward looking forecasts. The long-term projections for 2025-2045 predict a continuous increase in MSW volume. The main drivers of this growth include rising urbanization, population growth, economic expansion, and changes in lifestyle. Notably, the acceleration in waste generation after 2030 stands out. By 2045, the annual MSW volume is estimated to reach approximately 825,929 tons (see Figure 11 - red column). This result highlights the need for serious long-term planning of waste management strategies in Şırnak province. Table 6 shows the actual, training, test, and forecasted MSW quantities for the period 2007-2045 using the BiLSTM model.

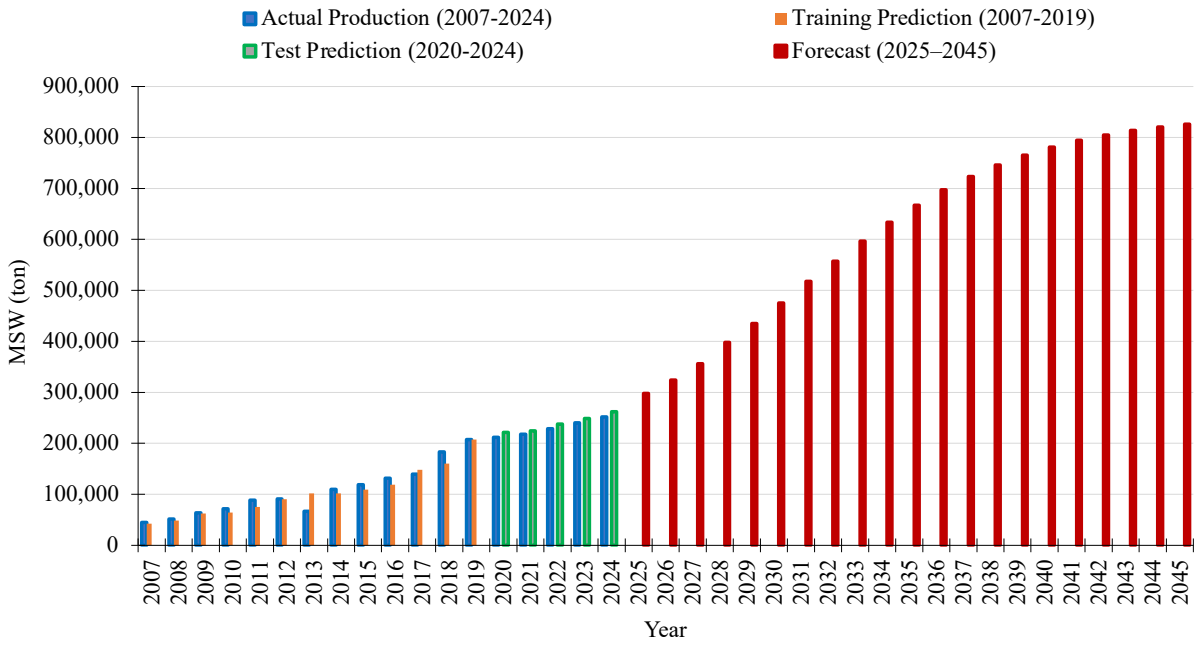

Figure 11. Column chart of actual, training, test, and future predicted MSW quantity results for the 2007-2045 period using the BiLSTM model.

Table 6. Actual, training, test, and forecasted MSW quantities (2007-2045) using the BiLSTM model.

Year	Ton of MSW			
	Actual Production	Training Prediction	Test Prediction	Forecast (2025-2045)
2007	44,673	42,636	-	-
2008	51,821	48,567	-	-
2009	63,725	62,478	-	-
2010	71,821	64,205	-	-
2011	88,544	75,471	-	-
2012	90,709	90,553	-	-
2013	66,658	102,171	-	-
2014	109,923	102,168	-	-
2015	118,936	108,966	-	-
2016	131,621	118,961	-	-
2017	139,255	147,999	-	-
2018	183,133	160,416	-	-
2019	207,238	207,238	-	-
2020	211,676	-	221,238	-
2021	217,716	-	224,676	-
2022	228,602	-	237,716	-
2023	240,032	-	248,602	-
2024	252,033	-	262,033	-
2025	-	-	-	298,090
2026	-	-	-	324,062

2027	-	-	-	356,296
2028	-	-	-	398,185
2029	-	-	-	435,035
2030	-	-	-	475,306
2031	-	-	-	517,475
2032	-	-	-	557,244
2033	-	-	-	596,378
2034	-	-	-	633,372
2035	-	-	-	666,847
2036	-	-	-	697,043
2037	-	-	-	723,505
2038	-	-	-	746,141
2039	-	-	-	765,305
2040	-	-	-	781,246
2041	-	-	-	794,327
2042	-	-	-	804,978
2043	-	-	-	813,568
2044	-	-	-	820,446
2045	-	-	-	825,929

Similar studies have also shown that BiLSTM models achieve high accuracy in time series data. For example, in a study by Liu et al. [6], it was reported that BiLSTM-based models produced lower MAPE values compared to classical LSTM and GRU architectures. This demonstrates that bidirectional contextual learning provides advantages, especially for MSW forecasts with complex and variable structures. Furthermore, the results obtained with the model configuration used in this study, which achieved a low error rate, are consistent with the parameter ranges suggested in previous literature. The forecasts made specifically for Şırnak province are important for developing applicable strategies at the regional level and indicate that this model can be adapted for similar regional studies.

The obtained results demonstrate that the BiLSTM model performs quite successfully in forecasting MSW based on historical data. The low error rate supports the model's reliability as a tool for predicting future waste quantities. However, the fact that only past MSW data were used in the forecasts excluding external factors such as population growth, economic development rates, or seasonal fluctuations can be considered a potential area for improvement in future studies.

In addition, the upward trend projected until 2045 highlights the need to improve waste management infrastructure, increase recycling rates, and enhance public awareness. For

policymakers, these findings can serve as a guide for strategic planning and the development of sustainable environmental policies.

3.2. CH_4 Gas, Electricity Energy Production Potential and Plant Capacity

In this study, the MSW quantities forecasted for the 2025-2045 period using the BiLSTM model were converted into CH_4 production potential using the LandGEM software. The LandGEM model is a widely accepted and validated tool in the literature for estimating CH_4 production resulting from the biological decomposition of waste. In line with this model, it was assumed that 75% of the generated CH_4 could be effectively captured, and the capturable CH_4 volume was calculated accordingly. This approach reflects a more realistic estimate of energy production potential by accounting for practical losses in real world applications.

According to the analysis results, CH_4 production from MSW in 2025 is estimated to be approximately 2,475,547 m^3, with a capturable volume of 1,856,660 m^3. By 2045, these values are projected to reach 6,861,036 m^3 and 5,145,777 m^3, respectively (Figure 12). Over the 21 year period, an approximate 64% increase in CH_4 production is observed. In total, cumulative CH_4 production during this period is calculated to be about 108.15 million m^3, with approximately 81.11 million m^3 being capturable. These figures are highly significant for long-term CH_4 gas management and energy recovery planning.

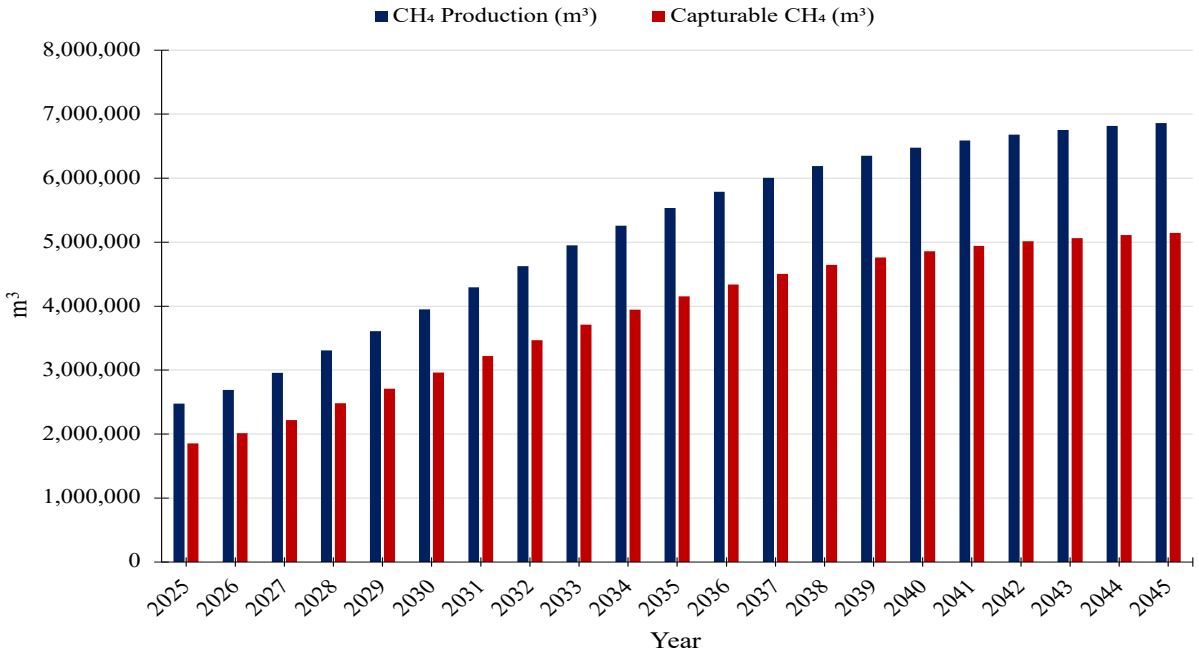

Figure 12. Annual CH_4 production and capturable CH_4 volumes (2025-2045).

Based on the annual capturable CH_4 volumes calculated from LandGEM outputs, the potential EEP and required plant capacity were estimated. For the year 2025, the EEP potential is approximately 5,157 MWh/year, and the required plant capacity is about 0.59 MW. By 2045, these values are projected to rise to 14,315 MWh/year and 1.63 MW, respectively (Figure 13). The estimated total EEPP for the period 2025-2045 is approximately 225,478 MWh (~225.4 GWh).

These findings indicate that if a waste to energy facility is to be established within the next 20 years, it should have a minimum capacity of 1.63 MW. However, to ensure safe operation and prepare for potential increases, it is recommended that the plant capacity be planned above this value. Additionally, the calculations assume continuous operation throughout the year, which necessitates consideration of factors such as maintenance, backup systems, and operational reliability.

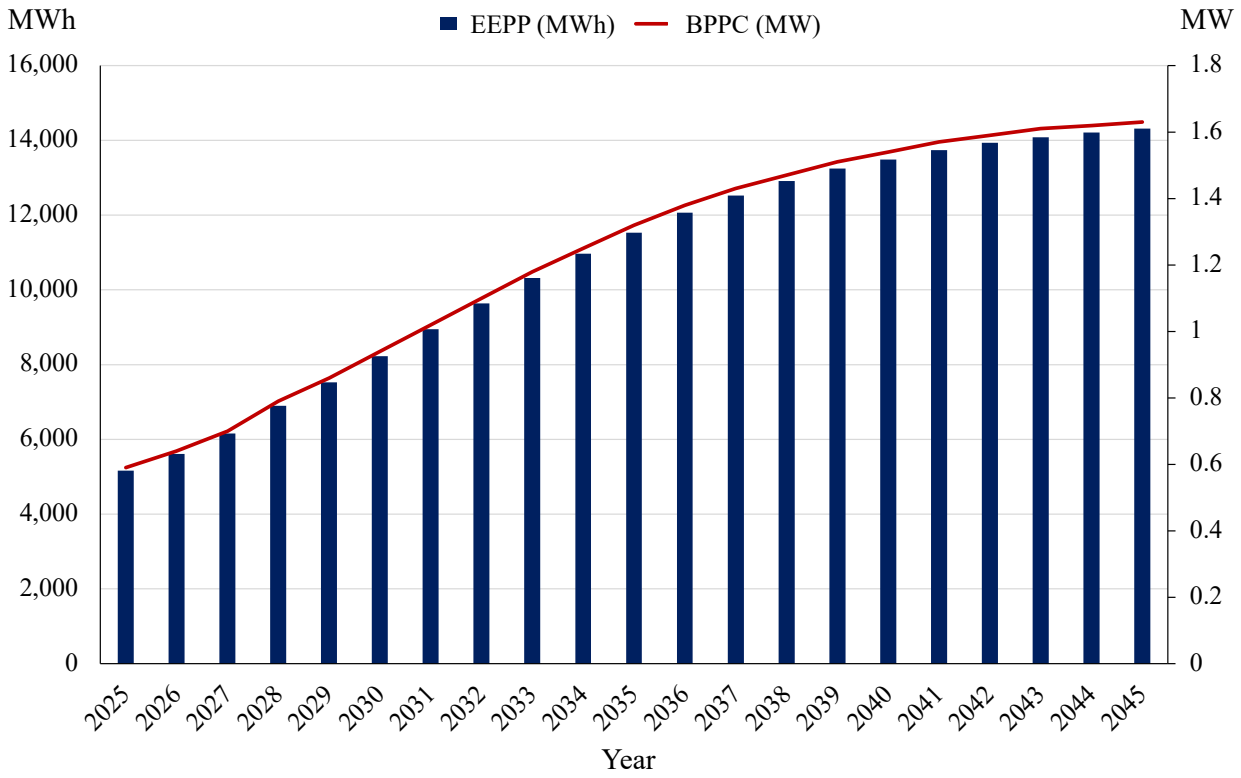

Figure 13. Variation in EEPP and BPPC (2025-2045).

3.3. Impact on Greenhouse Gas Emissions

In this study, the impact of electricity generated from biogas on greenhouse gas emissions was evaluated. The analysis compared the CO_2eq. emissions resulting from electricity produced using MSW derived biogas with those from producing the same amount of electricity using fossil fuels

(natural gas, oil, coal). The emission factors recommended by the IPCC for CO_2eq. were used in the calculations.

According to the results, the use of biogas for energy production can prevent a significant amount of greenhouse gas emissions annually. For example, in 2025, EEPP of approximately 5,157 MWh from biogas (BCO_2eq.) would result in only 258 tons of CO_2eq. emissions, whereas generating the same amount of electricity from Natural Gas ($NGCO_2$eq.), Oil (OCO_2eq.), and Coal (CCO_2eq.) would produce 2,114 tons, 3,780 tons, and 4,579 tons of CO_2eq. emissions, respectively. Considering the average fossil fuel based emissions (Avg. Avoided CO_2eq.), it is estimated that around 2,425 tons of CO_2eq. emissions can be avoided in 2025 (Figure 14).

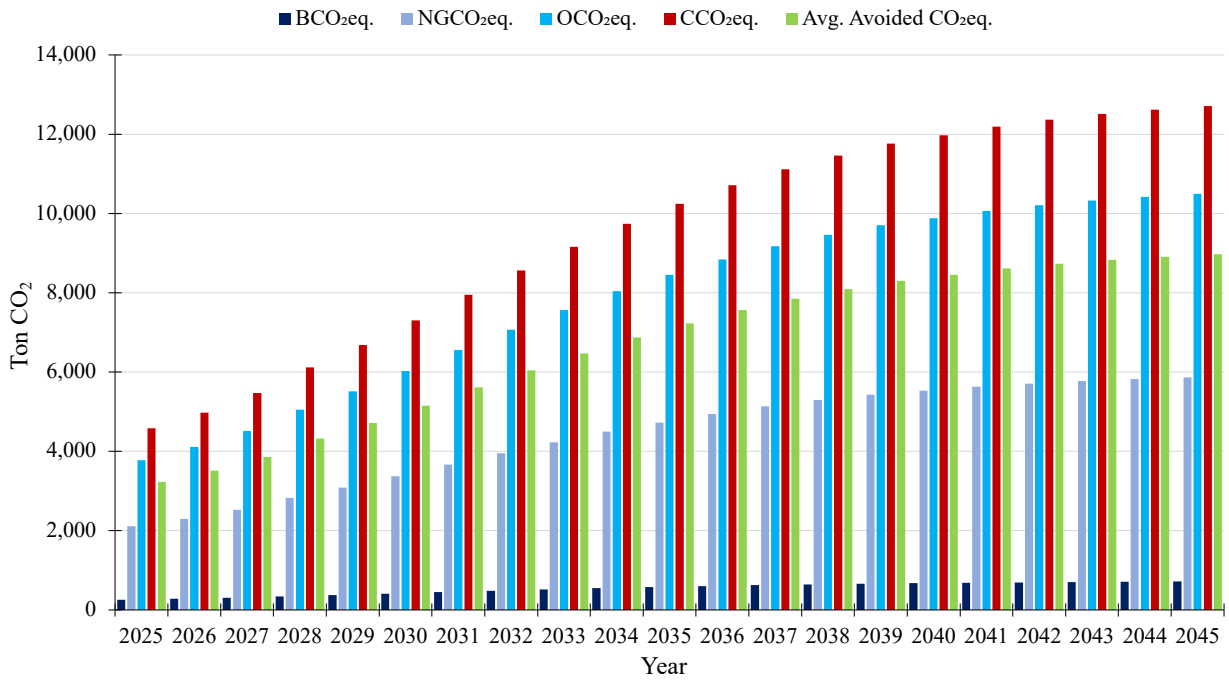

Figure 14. Comparison of CO_2eq. emissions from biogas and fossil fuel based EEP (2025-2045).

Long-term analyses indicate that between 2025 and 2045, biogas based EEP could prevent a total of approximately 141,375 tons of CO_2eq. emissions originating from fossil fuels. This value highlights that waste based renewable energy production in the Şırnak province is strategically important not only for energy supply security but also for combating climate change.

4. CONCLUSIONS AND RECOMMENDATIONS

In this study, the MSW quantities for the Şırnak province during the period 2025-2045 were predicted using the BiLSTM DLr model. During the parameter optimization process, various

hyperparameter combinations were tested, and the model achieving the lowest MAPE (3.83%) was selected as the best performer. Additionally, the model's generalization capability was validated with a 5-fold cross-validation, resulting in an average MAPE of 7.99%. These results demonstrate that the BiLSTM model can produce highly accurate predictions and can be confidently used for MSW forecasting based on time series data.

According to the model's forecasts, the annual MSW amount in Şırnak is expected to increase steadily, reaching approximately 825,929 tons by 2045. This trend can be attributed to population growth, rising urbanization rates, economic development, and changing consumption habits in the region. The long-term prediction highlights the need to reassess waste management systems in terms of capacity and infrastructure.

Based on the BiLSTM prediction results and subsequent LandGEM model analyses, CH_4 gas production is estimated to rise from about 2.47 million m^3 in 2025 to 6.86 million m^3 by 2045. During the same period, the volume of capturable CH_4 is expected to increase from 1.86 million m^3 to 5.14 million m^3. Over the 2025-2045 period, a total CH_4 production of approximately 108.15 million m^3 and capturable CH_4 volume of 81.11 million m^3 are projected. This indicates a significant growth potential for biogas based energy production. Calculations based on capturable CH_4 suggest that EEPP will increase from 5,157 MWh/year in 2025 to 14,315 MWh/year in 2045. Overall, an estimated total EEP of around 225,478 MWh is expected between 2025 and 2045. This implies that waste to energy facilities should be planned with a minimum capacity of 1.63 MW.

Based on the findings of this study, the following recommendations are proposed:

- The accuracy of predictions can be improved by including external variables such as population, economic growth, and seasonality in the BiLSTM model.
- Regular data collection and model updates should be performed for long-term waste management and energy planning.
- Local authorities should develop supportive policies for biogas energy use to reduce the carbon footprint and minimize greenhouse gas impacts.
- Waste management regulations and incentives should be updated in light of technological advancements, and economic models encouraging biogas production should be established.

- Municipalities and local administrations should enhance waste collection and disposal infrastructure to accommodate increasing MSW quantities, with a particular focus on investing in recycling and biogas facilities.
- Public awareness campaigns should be promoted to reduce waste generation and encourage sustainable waste management strategies.

ACKNOWLEDGMENT

The authors would like to express their gratitude to the editors and anonymous reviewers of the International Journal of Energy Studies for their valuable suggestions that helped improve the article.

DECLARATION OF ETHICAL STANDARDS

The authors of the paper submitted declare that nothing which is necessary for achieving the paper requires ethical committee and/or legal-special permissions.

CONTRIBUTION OF THE AUTHORS

Ceylan Üren: Acquisition of data, analysis, writing original draf, editing the whole manuscript.
Edip Taşkesen: Supervising the whole process.

CONFLICT OF INTEREST

There is no conflict of interest in this study.

REFERENCES

[1] Karak T, Bhagat RM, Bhattacharyya P, Municipal solid waste generation, composition, and management: the world scenario. Critical Reviews in Environmental Science and Technology 2012; 42(15):1509-1630.

[2] Valavanidis A. Global municipal solid waste (MSW) in crisis: two billion tonnes of MSW every year, a worrying Worldwide environmental problem [Online]. Available: http://chem-tox-ecotox.org/, Accessed: Jan. 17, 2023.

[3] Singh RP, Tyagi VV, Allen T, Ibrahim MH, Kothari R. An overview for exploring the possibilities of energy generation from municipal solid waste (MSW) in Indian scenario. Renewable and Sustainable Energy Reviews 2011; 15(9):4797-4808.

[4] Kaur A, Bharti R, Sharma R. Municipal solid waste as a source of energy. Materials Today: Proceedings 2023; 81(Pt 2):904-915.

[5] Arli F, Celebi N, Salimi K. The role of an ultra-thin carbon layer in enhancing solar water-splitting performance of Z-scheme ZnO@MOF-5/C photoanodes. Colloids Surf A Physicochem Eng Asp 2025; 720(137112):1-14.

[6] Liu B, Han B, Liang X, Liu Y. Hydrogen production from municipal solid waste: Potential prediction and environmental impact analysis. International Journal of Hydrogen Energy 2024; 52:1445-1456.

[7] Zheng L, et al. Preferential policies promote municipal solid waste (MSW) to energy in China: Current status and prospects. Renewable and Sustainable Energy Reviews 2014; 36:135-148.

[8] Hoang AT, et al. Perspective review on Municipal Solid Waste-to-energy route: Characteristics, management strategy, and role in circular economy. Journal of Cleaner Production 2022; 359:131897.

[9] Asamoah B, Nikiema J, Gebrezgabher S., Odonkor S., Njenga M., A review on production, marketing and use of fuel briquettes, ICRAF, Colombo, Sri Lanka, 2016.

[10] Malav LC, Yadav K K, Gupta N, Kumar S, Sharma GK, Krishnan S, Rezania S, Kamyab H, Pham QB, Yadav S, Bhattacharyya S, Yadav VK, Bach QV. A review on municipal solid waste as a renewable source for waste-to-energy project in India: Current practices, challenges, and future opportunities. Journal of Cleaner Production 2020; 277:123227.

[11] Bulbul S, Ertugrul G, Arli F. Investigation of usage potentials of global energy systems. International Advanced Researches and Engineering Journal 2018; 2(1):58-67.

[12] Dahlquist E, Biomass as Energy Source: Resources, Systems and Applications (Vol. 3). New York: CRC Press, Taylor & Francis Group, 2012.

[13] ACT Government Recyclopedia, "Landfill gas to energy," Government of the Australian Capital Territory. [Online]. Available: https://www.cityservices.act.gov.au/. Accessed: Jun. 20, 2025.

[14] Kantar O, Kilimci ZH. Deep learning based hybrid gold index (XAU/USD) direction forecast model. Journal of the Faculty of Engineering and Architecture of Gazi University 2023; 38(2):1117-1128.

[15] Uyar R, Özdemir D. Deprem şiddet tahmini için derin öğrenme yöntemlerinin karşılaştırılması ve model önerisi. Afyon Kocatepe Üniversitesi Fen ve Mühendislik Bilimleri Dergisi 2025; 25(3):522-534.

[16] Çetin Ö, Isık AH. Derin öğrenme ile güneş enerjisi santrallerinde aylık elektrik üretim tahmini. Mehmet Akif Ersoy Üniversitesi Fen Bilimleri Enstitüsü Dergisi 2022; 13(1):382-387.
[17] J. Zhang, P. Wang, R. Yan, and R. X. Gao, Long short-term memory for machine remaining life prediction. Journal of Manufacturing Systems 2018; 48(C): 78-86.
[18] Xu W, Jiang Y, Zhang X, Li Y, Zhang R, Fu G. Using long short-term memory networks for river flow prediction. Hydrology Research 2020; 51(6):1358-1376.
[19] Song X, Liu Y, Xue L, Wang J, Zhang J, Wang J, Jiang L, Cheng Z. Time-series well performance prediction based on Long Short-Term Memory (LSTM) neural network model. Journal of Petroleum Science and Engineering 2020; 186:106682.
[20] Hua Y, Zhao Z, Li R, Chen X, Liu Z, Zhang H. Deep learning with long short-term memory for time series prediction. IEEE Communications Magazine 2019; 57(6):114-119.
[21] Alizadegan H, Rashidi Malki B, Radmehr A, Karimi H, Ilani M A. Comparative study of long short-term memory (LSTM), bidirectional LSTM, and traditional machine learning approaches for energy consumption prediction. Energy Exploration & Exploitation 2025; 43(1):281-301.
[22] Hochreiter S. Untersuchungen zu dynamischen neuronalen Netzen (Ph.D. dissertation). Technische Universität München, München, Germany; 1991.
[23] Hochreiter S, Schmidhuber J. Long short-term memory. Neural Comput 1997; 9(8):1735-1780.
[24] Berus Y, Benteşen Yakut Y. Derin Öğrenme (1D-CNN, RNN, LSTM, BiLSTM) ile Enerji Tüketim Tahmini: Diyarbakır AVM Örneği. DÜMF Mühendislik Dergisi 2024; 15(2):311-322.
[25] Ozbayoglu AM, Gudelek MU, Sezer OB. Deep learning for financial applications: A survey. Applied Soft Computing 2020; 93:106384.
[26] Li Y, Du G, Xiang Y, Li S, Ma L, Shao D, Wang X, Chen H. Towards Chinese clinical named entity recognition by dynamic embedding using domain-specific knowledge. Journal of Biomedical Informatics 2020; 106:103435.
[27] Guo J, Liu M, Luo P, Chen X, Yu H, Wei X. Attention-based BILSTM for the degradation trend prediction of lithium battery. Energy Reports 2023; 9(2):655-664.
[28] KTB, "Şırnak-Genel Bilgiler," Kültür ve Turizm Bakanlığı Turizm İstatistikleri, Şırnak İl Kültür ve Turizm Müdürlüğü. Accessed: May 18, 2025. [Online].
[29] TÜİK, "Merkezi Dağıtım Sistemi MEDAS," Türkiye İstatistik Kurumu. Accessed: Jun. 18, 2025. [Online]. Available: https://biruni.tuik.gov.tr/medas/?locale=tr
[30] "Faaliyet Raporu," Şırnak Belediyesi. Accessed: Jun. 19, 2025. [Online]. Available: https://www.sirnak.bel.tr/

[31] Niu D, Wu F, Dai S, He S, Wu B. Detection of long-term effect in forecasting municipal solid waste using a long short-term memory neural network. Journal of Cleaner Production 2021; 290:125187.
[32] Gers F A, Schmidhuber J, Cummins F. Learning to forget: Continual prediction with LSTM. Neural Compu. 2000; 12(10):2451-2471.
[33] Liu B, Han Z, Li J, Yan B. Comprehensive evaluation of municipal solid waste power generation and carbon emission potential in Tianjin based on Grey Relation Analysis and Long Short Term Memory. Process Safety and Environmental Protection 2022; 168:918-927.
[34] Liu B, Zhang L, Wang Q. Demand gap analysis of municipal solid waste landfill in Beijing: Based on the municipal solid waste generation. Waste Management 2021; 134:42-51.
[35] da Silva DG, de M. Meneses AA. Comparing Long Short-Term Memory (LSTM) and bidirectional LSTM deep neural networks for power consumption prediction. Energy Reports 2023; 10:3315-3334.
[36] Vu HL, Ng KTW, Richter A, An C. Analysis of input set characteristics and variances on k-fold cross validation for a Recurrent Neural Network model on waste disposal rate estimation. Journal of Environmental Management 2022; 311:114869.
[37] Xiao S, Dong H, Geng Y, Tian X, Liu C, Li H. Policy impacts on Municipal Solid Waste management in Shanghai: A system dynamics model analysis. Journal of Cleaner Production 2020; 262:121366.
[38] Shapiro-Bengtsen S, Andersen FM, Münster M, Zou L. Municipal solid waste available to the Chinese energy sector - Provincial projections to 2050. Waste Management 2020; 112:52-65.
[39] Krause M, Thorneloe S. Landfill Gas Emissions Model (LandGEM) Version 3.1 User Manual and Tool. Washington; 2024.
[40] Cudjoe D, Han MS, Chen W. Power generation from municipal solid waste landfilled in the Beijing-Tianjin-Hebei region. Energy 2021; 217:119393.
[41] Sil A, Kumar S, Kumar R. Formulating LandGem model for estimation of landfill gas under Indian scenario. International Journal of Environmental Technology and Management (IJETM) 2014; 17:239-299.
[42] Ayodele TR, Ogunjuyigbe ASO, Alao MA. Life cycle assessment of waste-to-energy (WtE) technologies for electricity generation using municipal solid waste in Nigeria. Applied Energy 2017; 201:200-218.
[43] Assamoi B, Lawryshyn Y. The environmental comparison of landfilling vs. incineration of MSW accounting for waste diversion. Waste Management 2012; 32(5):1019-1030.

[44] Ayodele TR, Ogunjuyigbe ASO, Alao MA. Economic and environmental assessment of electricity generation using biogas from organic fraction of municipal solid waste for the city of Ibadan, Nigeria. Journal of Cleaner Production 2018; 203:718-735.

[45] Ogunjuyigbe ASO, Ayodele TR, Alao MA. Electricity generation from municipal solid waste in some selected cities of Nigeria: An assessment of feasibility, potential and technologies. Renewable and Sustainable Energy Reviews 2017; 80:149-162.

[46] IPCC. Energy (2006 IPCC Guidelines for National Greenhouse Gas Inventories Volume 2). Geneva: Intergovernmental Panel on Climate Change; 2006. [Online]. Available: https://www.ipcc-nggip.iges.or.jp/. Accessed: Jun. 21, 2025.

[47] WNA. Comparison of Lifecycle Greenhouse Gas Emissions of Various Electricity Generation Sources. London: World Nuclear Association; 2011. [Online]. Available: https://world-nuclear.org/. Accessed: Jun. 21, 2025.

[48] Sak T, Gönen Ç, Kara EE. Niğde ilinde güneş enerjisi santrallerinin yaygınlaştırılması ve sera gazı emisyonlarının azaltılmasının potansiyeli. Fırat Üniversitesi Mühendislik Bilimleri Dergisi 2019; 31(2):327-335.

[49] Chum H, Faaij A, Moreira J, Berndes G, Dhamija P, Dong H, Gabrielle B, Goss Eng A, Lucht W, Mapako M, Masera Cerutti O, McIntyre T, Minowa T, Pingoud K. Bioenergy. In: Edenhofer O, Pichs-Madruga R, Sokona Y, Seyboth K, Matschoss P, Kadner S, Zwickel T, Eickemeier P, Hansen G, Schlömer S, von Stechow C, editors. IPCC special report on renewable energy sources and climate change mitigation. Cambridge, U.K. and New York, NY, USA: Cambridge University Press; 2011.